A pendulum in a flowing soap film

M. M. Bandi, A. Concha, R. Wood, and L. Mahadevan

Additional information on Phys. Fluids

A pendulum in a flowing soap film

M. M. Bandi,[1,a)] A. Concha,[1,b)] R. Wood,[1] and L. Mahadevan[1,2]

[1]*School of Engineering and Applied Sciences, Harvard University, Cambridge, Massachusetts 02138, USA*

[2]*Department of Physics, Harvard University, Cambridge, Massachusetts 02138, USA*

We consider the dynamics of a pendulum made of a rigid ring attached to an elastic filament immersed in a flowing soap film. The system shows an oscillatory instability whose onset is a function of the flow speed, length of the supporting string, the ring mass, and ring radius. We characterize this system and show that there are different regimes where the frequency is dependent or independent of the pendulum length depending on the relative magnitude of the added-mass. Although the system is an infinite-dimensional, we can explain many of our results in terms of a one degree-of-freedom system corresponding to a forced pendulum. Indeed, using the vorticity measured via particle imaging velocimetry allows us to make the model quantitative, and a comparison with our experimental results shows we can capture the basic phenomenology of this system. © *2013 American Institute of Physics.* [http://dx.doi.org/10.1063/1.4800057]

A systematic study of the simple pendulum commenced with the observations by Galileo and others, heralding their employment as timekeepers.[1] The mechanism driving the oscillations of a pendulum is the competition between an orienting field and a periodic variable, and is ubiquitous in a range of phenomena in physics.[2] Mathematically, the dynamics of such processes occur on a circle;[3] physically, the effects of forcing, damping, and spatial coupling make the behavior of the pendulum nontrivial. Here we study one such variant using a combination of experiment and theory—the dynamics of an annular ring that is suspended by a string and immersed in a moving quasi-2D fluid represented by a gravity driven soap film tunnel (Fig. 1). The ambient quasi-2D flow within the soap film hydro-dynamically forces the pendulum, causing it to oscillate above a critical flow speed like a flapping flag.[4] We consider the onset of the oscillatory behavior and the resulting frequency as a function of the inertial and hydrodynamic parameters in the system.

Our experimental setup consisted of a soap film[5] (see Fig. 1(a)) flowing through an entry nozzle (1 mm diameter) between two laterally spaced nylon wires (diameter 0.5 mm, spacing $9 \leq W \leq 12$ cm, working height 1.0 m), tensioned by a heavy weight immersed in a bottom reservoir containing soap solution of density ρ_f (2.5% Dawn soap in distilled water). The solution is steadily pumped to a top reservoir and maintained at constant level ~0.2 m above the nozzle via a level-sensitive drainage mechanism (see Fig. 1(a)). As the film height and width are much larger than its thickness ($h \sim 10 \, \mu$m), we have approximately 2D flow. Our pendulum consists of a thin fiber (silk or nylon) with a bending stiffness B_0, linear mass density λ, length l, and mass $M_s = \lambda l$ glued at one end to a stiff polymer ring and introduced at the other end into the film at a point P using a pippete that does not penetrate the soap film and thus does not have a wake. The ring (thickness $t = 100 \, \mu$m) was laser cut from Polyethylene terephthalate and Kapton sheets of density ρ_R with internal radius R_i, external radius R, and mass M_R. The pivot P was located 0.5 m downstream from the nozzle to allow for the soap solution to reach a steady state with an average velocity $V = 0.4$–1.5 m/s.

---

a)Present address: Collective Interactions Unit, OIST Graduate University, 1919-1 Tancha, Onna-son, Kunigami-gun, Okinawa 904-0495, Japan.

b)Present address: School of Engineering and Sciences, Adolfo Ibañez University, Diagonal las torres 2640, Peñalolen, Santiago, Chile.

    25, 041702-1
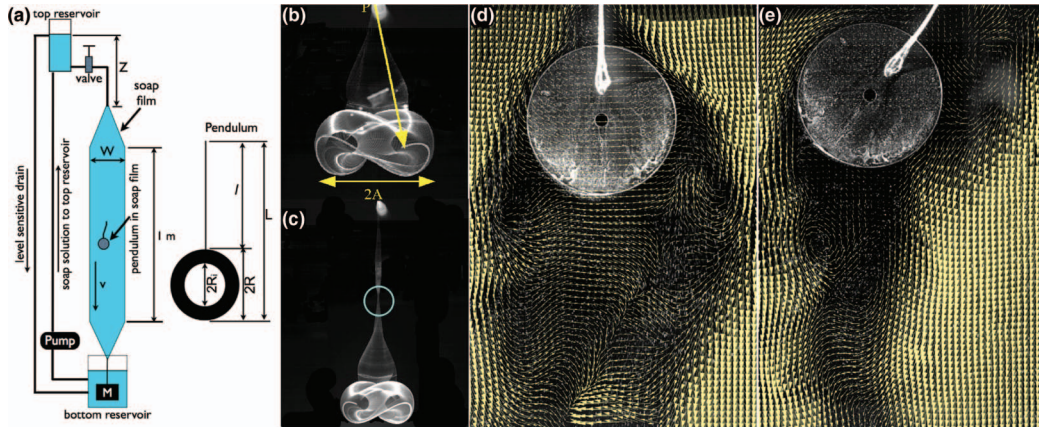
FIG. 1. (a) Schematic of experimental setup: Soap solution at constant pressure head flows through a nozzle between two parallel nylon wires that are a width W apart and over a length 1 m to form a soap film. An annular ring of external radius $R = 1.1 \times 10^{-2}$ m hangs from a flexible string that is pivoted outside the soap film. (b) For a given flow rate, the pendulum exhibits oscillatory motion above a critical length L_c. Multiple images of oscillations over several periods record the pendulum amplitude A. (c) A longer pendulum exhibits more complex oscillations, such as one with a node as marked with the blue circle. (d) Velocity field superposed on raw images shows when it is vertical and (e) when it is at its extremal position (enhanced online) [URL: http://dx.doi.org/10.1063/1.4800057.1] [URL: http://dx.doi.org/10.1063/1.4800057.2].

In Figures 1(b) and 1(c) we show a superposition of images of the driven pendulum for two different string lengths; the short one oscillates without a node, while the longer one has a node. We quantified the fluid flow and pendulum dynamics using two different methods involving high speed digital imaging at 3500–5500 fps. In the first method, pendulum oscillations were captured with a high-speed camera (Phantom v7.3) under diffuse (non-coherent) illumination and the images were analyzed to determine the oscillation frequency and amplitude of motion. In the second method, hollow glass particles (diameter 8 μm, density 1.05 g/cm^3) were suspended in the soap solution and a laser (4W, 528 nm) sheet illuminated a rectangular section of the film (width W and length of 6–8 cm) in the vicinity of the pendulum to capture light scattered off the glass particles. Particle Imaging Velocimetry (PIV) algorithms were employed to construct the velocity field around the pendulum (Figs. 1(d) and 1(e)) and capture the motion of the fluid and the moving ring. In Figures 1(d) and 1(e) we show this velocity field in the wake of the pendular ring at its central and extreme positions; both these show the presence of vortical structures with a size comparable to that of the ring. We see that the motion of the system shows two rotational modes: one that corresponds to the oscillatory motion of the ring and string pendulum about the pivot where the string enters the soap film, and the other associated with the motion of the ring as it pivots at the end of the string. These modes are coupled: indeed their frequencies are the same. However, as we will see, a single degree of freedom model is sufficient to explain the salient features of the system dynamics.

Unlike the simple pendulum, which can be described in terms of a balance between inertia and gravity and mediated by fluid damping, here we also have to account for the driving forces and torques from the flowing fluid. Then the balance of angular momentum for the fluid-driven pendulum about the out-of-plane $\hat{z}$ axis yields the equation of motion,

$$I\ddot{\theta} = [\vec{L}_{cm} \times (\vec{F}_d + M_P \vec{g}) + \vec{\tau}_v] \cdot \hat{z} - \nu\dot{\theta}. \tag{1}$$

Here, $\theta(t)$ is the angle that the string makes with the vertical, $\vec{\tau}_v$ is the torque on the ring arising from vortex shedding, $\vec{F}_d$ is the fluid drag, and $M_P \vec{g}$ is the weight of the ring. The fluid drag $|\vec{F}_d| = C_D \rho_f V^2 L h \sin(\theta)$, where $L \sim (l + R)$ (assuming that only the first mode is excited[6]), $\vec{L}_{cm}$ is the vector joining P to the pendulum's center of mass, M_P is the bare pendulum mass, and $\nu\dot{\theta}$ is the damping torque arising due to the effects of fluid viscosity. Here and elsewhere, we use the drag coefficient $C_D = 0.5$. The moment of inertia $I = (M_R + M_A + M_s)L_{cm}^2$ is the sum of three terms arising from the ring mass M_R, added mass $M_A \sim \rho_f (l + R)Ah$, where $A \sim L$ is the oscillation amplitude, and string mass M_s. Since these masses exhibit markedly different dependences on the
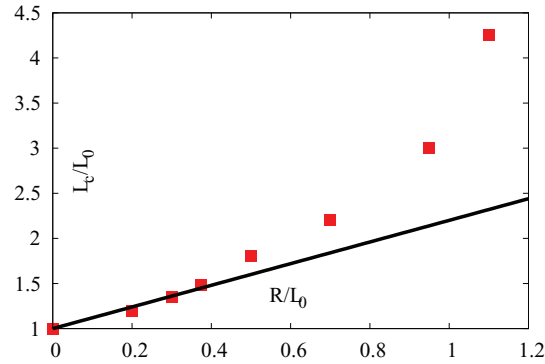
FIG. 2. Dimensionless critical length L_c/L_0 vs. dimensionless ring radius R/L_0, (where L_0 is the smallest length of a fiber without an attached ring that spontaneously oscillates in a flow) at constant mass M_R and flow rate, obtained experimentally (solid squares). The solid line corresponds to the best fit obtained from the first four points, with $L_c/L_0 = 1 + 1.2R/L_0$.

pendulum length, with $M_R \sim L^0$, $M_s \sim L^1$, and $M_A \sim L^2$, their relative contribution controls how the oscillation frequency of the pendulum scales with the pendulum length L.

At low flow velocities, or equivalently, when the fiber is short and/or the ring is heavy, the pendulum is stationary. However, once the length of the suspending fiber is longer than a critical length L_c, we see the onset of spontaneous oscillations. In the absence of the ring, the problem is similar to that of flag flutter. A scaling estimate for the critical length L_0 above which a bare string (without a ring at its end) is unstable to flutter follows from a competition between fluid forces and the elastic bending resistance of the string in the absence of gravity.[7] This yields $L_0 = \left(\frac{B_0}{\rho_f V^2 h} \right)^{\frac{1}{3}}$, where B_0 is the bending stiffness of the string, and V is the far field fluid speed. In the presence of a ring, three new effects arise—gravity which stabilizes the pendulum, tension in the string induced by fluid drag which also stabilizes the pendulum, and finally, low frequency vortex shedding from the ring that can destabilize the pendulum, unlike what typically happens in a flag. In Fig. 2, we show that L_c increases with the ring radius over the range $0.2 \leq R \leq 1.1$ cm. To understand this result qualitatively, we note that the pendulum spontaneously starts to oscillate when the torque induced by vortex shedding from the string-pendulum system overcomes the stabilizing forces that arise from gravity and fiber tension.

The various different regimes of oscillatory behavior pit inertia against the sum of various stabilizing and destabilizing influences. We start by ignoring the effects of gravity, and instead focus on the case when the fluid drag $\rho_f V^2(l + R)h \gg M_R g$. In the limit of a heavy ring at the end of a relatively long fiber where $R \leq l$, the moment of inertia about the pivot $I \sim (l + R)^2 M_R$. Then, balancing the rotary inertial torque $I\omega^2\theta \sim M_R(l + R)^2\omega^2\theta$ with the fluid-induced torque $\rho_f V^2(l + R)^2 h\theta$, we get

$$\omega \sim V\sqrt{\frac{\rho_f h}{M_R}},\tag{2}$$

i.e., the oscillation frequency for heavy rings is length independent, in contrast with the result for a simple pendulum. In Fig. 3(a) we show that this result is consistent with our experiments.

When the string mass exceeds the ring mass and added mass, i.e., $M_S > M_R, M_A$, our earlier result (2) remains valid, but with M_R replaced by $M_S \sim \lambda l$, so that

$$\omega \sim V\sqrt{\frac{\rho_f h}{\lambda l}}.\tag{3}$$
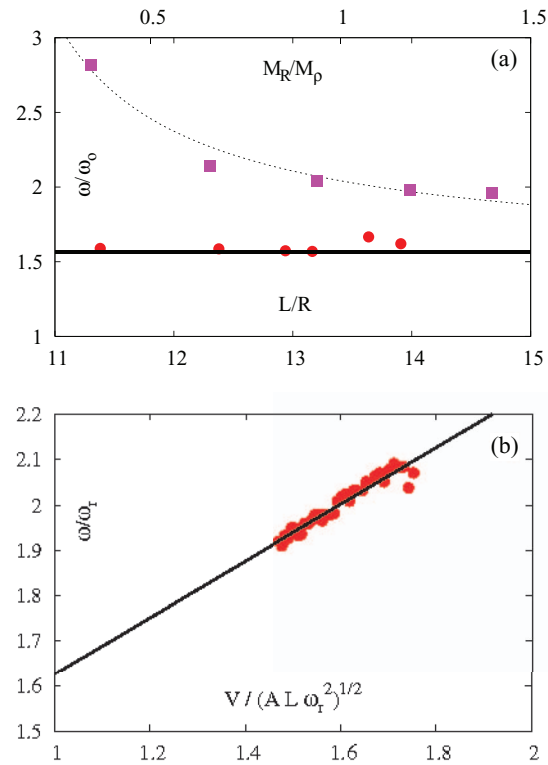
FIG. 3. (a) Dimensionless frequency ω/ω_0 vs. dimensionless length L/R (bottom horizontal axis) when $M_R > M_A$ ($M_R = 1.48 \times 10^{-4}$ kg). Experimental data are shown as solid circles and a fit based on Eq. (2) is shown as a solid line; $\omega_0 = 9.44$ s^{-1} is the natural frequency for a gravity pendulum of length $L = 10R$. Top horizontal axis shows the regime when $M_R < M_A$, with the ring radius held constant at $R = 1.1 \times 10^{-2}$ m while increasing mass M_R by adding plasticine, with $M_\rho = \pi R^2 \rho h$ being the mass of a disc of liquid of radius R. Experiment (solid squares) and theory fit (dashed line) from Eq. (4). (b) Dimensionless frequency ω/ω_r vs. rescaled velocity $V/(AL\omega_r^2)^{1/2}$ based on Eq. (4) in the added mass regime $M_A > M_R$ & M_s. Here $\omega_r = 19.08$ s^{-1} is the offset frequency corresponding to the mode where the ring oscillates around its pivot.

When $M_A \gg M_s, M_R$, the rotational inertia associated with the added mass is $\rho_f(l+R)^2 Ah\theta\omega^2$. Balancing this with the fluid torque $\rho_f V^2(l+R)h\theta$ yields

$$\omega \sim V\sqrt{\frac{1}{(l+R)A}}. \tag{4}$$

We see that for long strings, when $L \sim l + R \approx l$, the frequency $\omega \sim L^{-1/2}$, a regime previously observed for a flexible loop oscillating in a soap film.[8] In all cases, the effect of an increased tension in the string effectively stiffens it,[9] thus increasing the critical length, while the vortex shedding can trigger the resonant motion of the pendulum. Although we have couched our results in Eqs. (2)–(4), in terms of a frequency, we can immediately convert them to a dimensionless form in terms of a Strouhal number $St = \frac{\omega R}{V}$ for each regime, as in Ref. 10.

We now turn to explore the role of added mass from an experimental perspective complementing previous theoretical aspects in the study of flags.[7,11] We used thin rings with $(R - R_i) \sim 50\,\mu$m, and measured the oscillation frequency as a function of the rescaled velocity based on Eq. (4); in Fig. 3(b) we show that our experiments are in agreement with our minimal scaling theory. Further confirmation of our scaling law comes from extracting the prefactor in Eq. (4) from Fig. 3(b) which yields $V = 0.625$ m/s, a value close to that determined experimentally using PIV, $V_{PIV} = 0.69 \pm 0.15$ m/s. However, we note that as $V \to 0$ (equivalently as $L \to \infty$), there is a finite frequency offset ω_r in contrast with prior studies.[8] To understand this, we note that although there are at least two rotational modes in the system as discussed at the start and observable in our
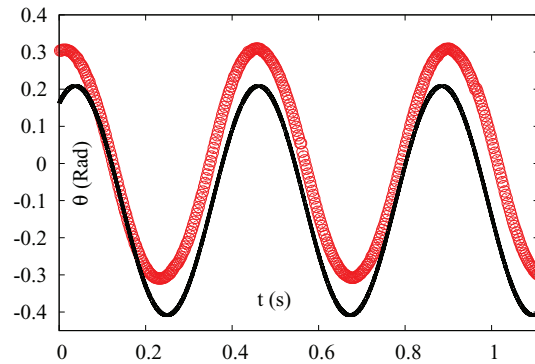
FIG. 4. Comparison between experimentally obtained angular dynamics shown with open circles (red) and the simple theory based on a driven oscillator model (solid black curve) given by Eq. (5) with the following parameters: $M_R = 0.12 \times 10^{-3}$ kg, $h = 10\,\mu$m, $V = 1$ m/s, $L = 5.5 \times 10^{-2}$ m, $\gamma = 80$ s^{-1}, $R = 1.1 \times 10^{-2}$ m. The numerical curve is intentionally offset by $\Delta\theta = 0.1$ for clarity.

experiments, as $L \to \infty$, the large added mass impedes the pendulum from oscillating as a whole. However, the remaining mode associated with the soft degree of freedom when the ring pivots about its attachment to the string persists. In the absence of flow, this mode has a resonant frequency $\omega_r = \sqrt{g/R}$, set by the balance between gravity and inertia; indeed it is this mode that is forced by the flowing fluid when the pendulum is very long. For rings of radius $R = 1.1$ cm, $\omega_r = 21.11$ s^{-1}, in agreement with the offset obtained from experiments $\omega_r = 19.08$ s^{-1}.

With the exception of the ring rotation mode just considered, we have so far assumed that gravity is negligible, a valid assumption for relatively fast flows. However, when gravity becomes comparable to fluid drag, there is a cross-over from fluid-driven to gravity-dominated oscillations. This transition occurs when the gravitational pendulum frequency $(g/(l+R))^{1/2} \sim (\rho_f V^2 h/M_R)^{1/2}$, the fluid-driven oscillation frequency given in Eq. (2), so that the cross-over ring mass $M_R^{cross} \sim \rho_f V^2(l+R)h/g$. For typical experimental values of $l+R \sim 10$ cm, V ~ 1 m/s, and $h \sim 10\,\mu$m, this yields $M_R^{cross} \sim 0.1$ g. To test our predictions in this regime, we increased the ring mass (M_R) by attaching dense plasticine at the center of the ring so that $M_R = 0.15$ g. When the length of the composite pendulum is in the range $12.5 \leq (l+R) \leq 15.5$ cm, and $V = 1.3$ m/s, the oscillation frequency ω = 13.20–13.70 s^{-1} in good agreement with our experimental data shown in Fig. 3(a).

We close with a brief discussion of the dynamics of the fluid-driven pendulum in the limit where the moment of inertia of the system is dominated by that of the ring. With $I = M_R L^2$ and $M_R \sim M_R^{cross}$, so that drag and gravity are comparable, the equation of motion (1) for the pendulum reads

$$ I\ddot{\theta} = -\left(M_R g L + \frac{\rho_f}{2}V^2 L^2 h\right)\sin\theta + \tau_v \sin\omega t - \nu\dot{\theta}, \qquad (5) $$

where the last two terms in Eq. (5) correspond to the torques from vortex shedding and viscous damping. The driving torque has an amplitude $\tau_v = \rho_f V \gamma R^2 h l$ (obtained by noting that the force due to fluid motion is $\rho_f V \Gamma h$, where $\Gamma \sim \gamma R^2$ is the circulation, where γ is the vorticity obtained from PIV measurements like those shown in Figs. 1(d) and 1(e)). The damping torque is obtained using experiments to measure the relaxation time of a short pendulum ($L < L_c$) that is perturbed and allowed to come to rest in a static soap film, and yields the result $\nu \sim 4I$ s^{-1}. In Fig. 4, we show the solution of Eq. (5), using the measured parameter values $\gamma \sim 80$ s^{-1}, and see that our experimental measurements for the amplitude of the driven pendulum are in good agreement with that of the theory with a single fitting parameter for the driving torque.

Our study of the fluid-driven pendulum in a soap film shows that there is a critical speed of the flow above which spontaneous oscillations arise. A simple scaling theory allows us to characterize the transition to oscillations, and is qualitatively consistent with our experiments. Furthermore, we find various regimes for the oscillation frequency by accounting for the relative contributions of the torques from the ring, filament, added mass, fluid drag, and gravity, also consistent with our

measurements. A model of a pendulum forced periodically by vortex shedding and damped by fluid drag allows us to quantitatively compare our results with observations, given the experimentally measured vorticity. Our findings complement earlier work on the dynamics of continuous objects such as strings and loops in flowing soap films, by focusing on the dynamics of an effectively low-dimensional system, but also raise questions about how different modes are coupled. Of particular interest is the coupling of the motion of the ring with its own wake, that causes it to bounce as it oscillates, presumably as a consequence of the impulsive loading due to vortex shedding when the ring is in its extremal positions, a problem worthy of further study.

[1] J. C. Taylor and F. V. Kersen, *Huygens' Legacy: The Golden Age of the Pendulum Clock* (Fromanteel Ltd., Isle of Man, 2004).

[2] G. Baker and J. Blackburn, *The Pendulum: A Case Study in Physics* (Oxford University Press, New York, 2005).

[3] L. D. Landau and E. M. Lifshitz, *Mechanics* (Pergamon Press, Oxford, 1960).

[4] J. Zhang, S. Childress, A. Libchaber, and M. Shelley, "Flexible filaments in a flowing soap film as a model for one-dimensional flags in a two-dimensional wind," Nature (London) **408**, 835 (2000).

[5] M. A. Rutgers, X. L. Wu, and W. B. Daniel, "Conducting fluid dynamics experiments with vertically falling soap films," Rev. Sci. Instrum. **72**, 3025 (2001).

[6] The presence of the flexible string implies that modes with multiple nodes can be observed (Fig. 1(d)), but here we focus only on the first mode, which is the one most commonly seen.

[7] M. Argentina and L. Mahadevan, "Fluid-flow-induced flutter of a flag," Proc. Natl. Acad. Sci. U.S.A. **102**, 1829 (2005).

[8] S. Jung, K. Mareck, M. Shelley, and J. Zhang, "Dynamics of a deformable body in a fast flowing soap film," Phys. Rev. Lett. **97**, 134502 (2006).

[9] The effect of tension in the fluttering instability renormalizes the bending stiffness so that $B_0 \to B_0 + TL^2$, where the tension $T \sim \rho_f V^2 Rh$.

[10] C. H. K. Williamson and R. Govardhan, "Vortex-induced vibrations," Annu. Rev. Fluid Mech. **36**, 413 (2004).

[11] L. Zhu and C. S. Peskin, "Simulation of a flapping flexible filament in a flowing soap film by the immersed boundary method," J. Comput. Phys. **179**, 452 (2002).